

# Electromagnetic and thermal homogenisation of an electrical machine slot

P. Romanazzi, J. Gyselinck, M. Bruna, D. A. Howey, *Member, IEEE*.

**Abstract**—In this paper we propose an original technique based on the finite element method to couple electromagnetic and thermal homogenisation of multiturn windings. The model accurately accounts for skin and proximity effects considering the temperature dependence of electrical resistivity. We validate the approach by modelling a reference electrical machine open slot with representative boundary conditions. The case study refers to a particular wire shape and winding periodic configuration but the method can be applied to any symmetrical wire shape. The homogenisation allows us to efficiently evaluate the hot-spot temperature within the slot. The solution provided by the homogenised model proves to be very accurate over a large range of frequencies, when compared to the results using a fine model where all the conductors are physically reproduced.

**Index Terms**— homogenisation, multiphysics, electrical machines, hot-spot temperature.

## I. INTRODUCTION

Energy conversion in electrical machines is affected by electromagnetic (EM) and mechanical losses. The losses are a function of a number of parameters, such as torque, rotational speed, control strategy, winding configuration, temperature, etc. Precise loss estimation allows for accurate thermal analysis of the machine, ensuring correct behaviour at any operational point, and a longer life, since the winding hot-spot temperature should always be kept lower than the threshold given by the winding insulation class [1]. Electrical machine windings are heated by resistive losses and ac effects can significantly increase the heat generation. A conductor exposed to a varying magnetic field from itself (skin effect) or neighbouring conductors (proximity effect) will exhibit a non-uniform current density  $\mathbf{J}$  and this needs to be quantified for accurate thermal modelling.

Usually, accurate loss computation may be achieved by numerical modelling such as solution of Maxwell's equations using the Finite Element (FE) method on a suitably refined mesh, accounting for every single wire (fine model). The temperature field is then solved on the same mesh by solving the heat equation using the losses from the EM simulation. Since conduction losses are dependent on temperature [2]–[4], the solution of the EM and thermal models should be coupled in order to obtain the total loss distribution, as a function of temperature, and the hot-spot temperature. The

This work was supported by the European Union: FP7 ITN Project 607361 ADEPT

P. Romanazzi and D. A. Howey are with the Department of Engineering Science, University of Oxford, Oxford, U.K. (e-mail: david.howey@eng.ox.ac.uk).

J. Gyselinck is with the BEAMS Department, Université Libre de Bruxelles (ULB), Belgium

M. Bruna is with the Mathematical Institute, University of Oxford, Oxford, U.K.

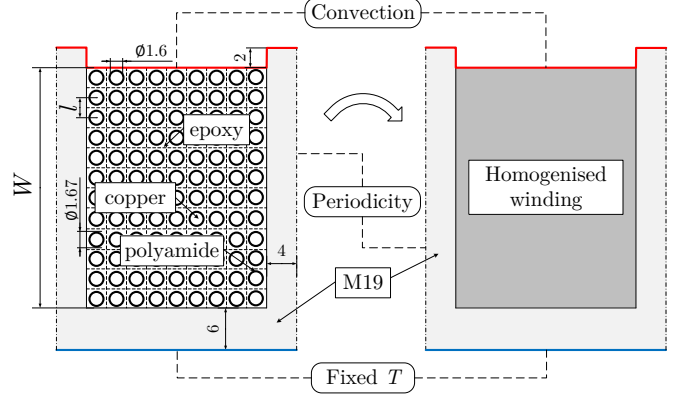


Fig. 1. Homogenisation of an open slot with 108 conductors disposed on a square lattice (12 layers of 9 wires),  $\lambda = 0.6$ ; dimensions are in [mm] and material properties are given in Table I

TABLE I  
REFERENCE MATERIAL PROPERTIES FOR THE ELECTROMAGNETIC AND THERMAL PROBLEMS

	Copper	Polyamide	Epoxy	M19
	$c$	$i$	$ep$	$m19$
$k$ [W/mK]	385	0.26	0.85	25
$c$ [J/kgK]	386	1000	1700	-
$d$ [kg/m <sup>3</sup> ]	8890	1440	1766	-
$\rho$ [ $\Omega$ m]	$\rho(T)$	0	0	0
$\mu$ [Hm]	$\mu_0$	$\mu_0$	$\mu_0$	$1200\mu_0$
$\epsilon$ [F/m]	$\epsilon_0$	$\epsilon_0$	$\epsilon_0$	$\epsilon_0$

computational burden related to this “brute force” approach is high. The homogenisation of the winding domain can significantly reduce the computational time; this is achieved by replacing the heterogeneous and periodic winding structure, i.e. insulated conductors bonded together with epoxy, with a homogeneous material made up of effective parameters, Fig. 1. It should be understood that model order reduction via homogenisation provides the macroscopic behaviour of the domain [5], ensuring the same level of accuracy provided by a fine model.

The homogenisation of the EM problem accounting for eddy currents introduces a frequency-dependent effective complex reluctivity for the homogenised winding domain and a frequency-dependent impedance for the external lumped circuit [6]. These parameters can be obtained from the solution of particular cell problems using FE assuming periodicity in

the original geometry, as we will show later. We can then analyse the homogenised winding in the frequency [7] or time [8,9] domain, with 2D [7,8] or 3D [9] geometries. The homogenisation can be applied also when 2 phases of a 3-phase machine are placed in the same slot [10].

In this work we extend the EM homogenisation method presented in [7] to account for the temperature dependence of the effective parameters in the homogenised EM model. As discussed in [11] the homogenisation of the thermal problem can be performed using analytical formulas, e.g. the Hashin and Shtrikman formula [12,13], or via measurement on suitable specimens [13,14]. However both these approaches have limitations, the first in terms of accuracy, as it is not able to accurately account for wire distribution and shape, whereas the second is not cost-effective. In this work the multiple-scales (MS) method [15] is employed because, as shown in the later sections, is able to provide a very accurate homogenisation with limited computations. The two homogenisation approaches are then coupled iteratively to obtain an overall solution of the EM and thermal behaviour of a reference electrical machine slot, Fig. 1. The resulting multiphysics homogenisation is shown to predict magnitude and location of the hot-spot temperature very accurately, by comparing it to the results given by a fully coupled fine model. All the numerical calculations shown in this paper were performed with COMSOL Multiphysics v5.2.

## II. ELECTROMAGNETIC HOMOGENISATION OF A WINDING

In this section we give an overview of the method presented in [7] for the homogenisation of the EM problem. The method is then extended to account for thermal effects.

When a sinusoidal current of frequency  $f$  (Hz) is injected into a multiturn winding, eddy currents are induced in the conductors. These are mainly a function of  $f$ , which may be expressed as the reduced frequency  $X = r\sqrt{f\pi\mu_0/\rho}$ , where  $r$ ,  $\rho$  and  $\mu_0$  are the conductor's radius, electrical resistivity and permeability respectively, and the skin depth  $\delta = \sqrt{2\rho/\omega\mu_0}$ , where  $\omega = 2\pi f$  (rad/s). Other parameters that affect these losses are wire shape and distribution, number of layers, filling ratio and temperature. A proper homogenisation of the winding should be able to reproduce the eddy-current effects even though the conductors are not physically modelled individually. In a fine model we calculate the distribution of  $\mathbf{J}$  in each wire with Maxwell's equations, using, e.g., the magnetic vector potential  $\mathbf{A}$  formulation, defined as  $\mathbf{B} = \nabla \times \mathbf{A}$  with  $\mathbf{B}$  the magnetic flux density. To homogenise the domain we need to obtain an effective complex reluctivity  $\nu_{prox}$  that accounts for the influence of an external magnetic field, i.e. proximity effect, where  $\nu = \mu^{-1}$ . To consider the skin effect, an effective impedance  $Z_{skin}$  is introduced in the lumped electrical circuit that feeds the winding.

Assuming that the conductors are connected in series and periodically distributed, e.g. on a square lattice, we can apply the method presented in [7] for the homogenisation of a multiturn winding in the frequency domain. The method exploits the orthogonality of the skin and proximity effect [16], which holds for symmetric conductors. To obtain the

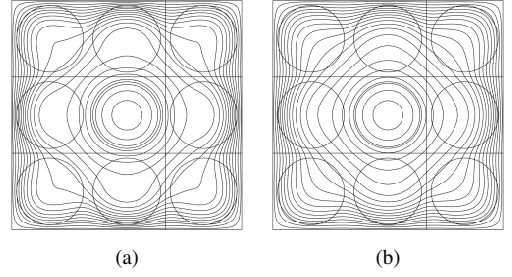


Fig. 2. Magnetic flux lines for the skin effect excited at 20 kHz for (a)  $T = 20^\circ\text{C}$  and  $X = 1.73$  or (b)  $T = 150^\circ\text{C}$  and  $X = 1.41$

effective quantities, the skin and proximity effects are excited separately on a limited number of elementary cells, Fig. 2; the former by injecting a unit current and imposing zero average flux density, the latter by removing the current and imposing a unit average horizontal flux density [7,8]. The number of elementary cells is chosen in order to balance accuracy and model complexity [7,17]. Fig. 2 shows the flux lines when the skin effect is excited in the elementary cells with a 20 kHz current at different temperatures. In Fig. 2 the elementary cells are distributed on a square lattice with a filling ratio  $\lambda = 0.6$ , where  $\lambda = \frac{\Omega_c}{\Omega}$ , with  $\Omega_c$  and  $\Omega$  being the conductor and unit cell surfaces respectively.

As shown in [7], we can express the effective complex reluctivity and effective impedance as

$$\nu_{prox} = q_B \nu_0 + j p_B \frac{\lambda r^2 \omega}{4\rho} \quad (1a)$$

$$Z_{skin} = p_I R_{DC} + j q_I \omega \frac{\mu_0 L}{8\pi \lambda} \quad (1b)$$

where  $R_{DC} = n_w L \rho / \Omega_c$  is the DC resistance at a certain temperature, with  $L$  the axial length of the domain,  $n_w$  the number of wires in the slot and  $j = \sqrt{-1}$ . The four dimensionless parameters  $p_I$ ,  $q_I$ ,  $p_B$  and  $q_B$  are obtained evaluating the complex power  $S = L \int_{\Omega} (\rho |J|^2 + j \omega \nu_0 |b|^2) d\Omega$  absorbed by the central cell of Fig. 2 when the skin effect ( $S_{skin}$ ) or the proximity effect ( $S_{prox}$ ) are excited. We then compute  $p_I$ ,  $q_I$ ,  $p_B$  and  $q_B$  with the following relations [7]

$$\frac{S_{prox}}{\Omega L |B|^2} = p_B \frac{\lambda r^2 \omega^2}{4\rho} + j q_B \omega \nu_0, \quad \frac{S_{skin}}{|I|^2} = Z_{skin} \quad (2)$$

where  $|Y|$  represents a r.m.s. value:  $|Y| = \sqrt{Y Y^*}$ .

We extend this technique to include the influence of temperature. It is well known that the temperature dependence of the electrical resistivity of a conductor can be approximated with

$$\rho(T) = \rho_0 (1 + \alpha(T - T_0)) \quad (3)$$

where  $T$  is temperature,  $\rho_0$  is the resistivity at the reference temperature  $T_0$  and  $\alpha$  is the temperature coefficient; e.g. for copper  $\rho = 1.68 \times 10^{-8} \Omega\text{m}$  at  $T_0 = 20^\circ\text{C}$  and  $\alpha = 0.003862^\circ\text{C}^{-1}$ . As shown in Table I the thermal conductivity of copper is very high compared to the thermal conductivity of the insulation and epoxy, thus we can assume that the temperature distribution within a conductor is always uniform. To analyse the parameters at, e.g.,  $T = 150^\circ\text{C}$ ,

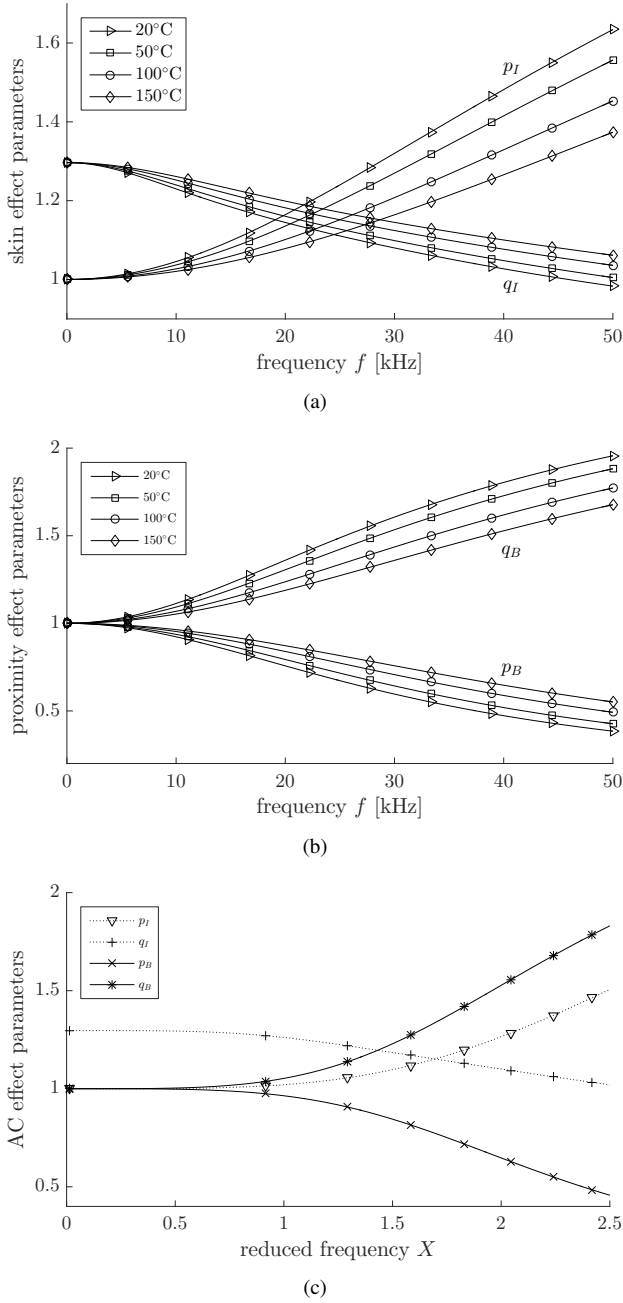


Fig. 3. Eddy-current parameters for wires on a square lattice with  $\lambda = 0.6$ ; (a) skin effect parameters  $p_I$  and  $q_I$  at various temperatures against frequency, (b) proximity effects  $p_B$  and  $q_B$  at various temperatures against frequency and (c)  $p_I$ ,  $q_I$ ,  $p_B$  and  $q_B$  against reduced frequency  $X = X(T)$

in the cell problems we adjust the conductor's resistivity to  $\rho = \rho(150^\circ\text{C})$  using (3), see Fig. 2(b). In Fig. 3(a) and 3(b)  $p_I$ ,  $q_I$ ,  $p_B$  and  $q_B$  are plotted as a function of  $f$ , for the case of  $\lambda = 0.6$ , distribution on a square lattice and various temperatures. The reduced frequency  $X = X(\rho(T))$  can be used to collapse the curves at different temperatures into a single line, as shown in Fig. 3(c). The multiphysics homogenisation is thus simplified, since we need to estimate a single set of four parameters only.

### III. THERMAL HOMOGENISATION OF THE WINDING

The temperature distribution within the winding can be obtained by solving the heat equation

$$C \frac{\partial T}{\partial t} = \nabla \cdot (k \nabla T) + \dot{q} \quad (4)$$

where  $C = cd$ , with  $c$  being specific heat capacity,  $d$  density, and  $k$  thermal conductivity. In our case, the internal heat generation  $\dot{q}$  is the coupling between the two problems as it comes from the EM computations. It is important to highlight that to properly solve the temperature field within a winding the wires' insulation has to be taken into account, because the insulation thermal conductivity can be significantly different from both the conductors and filling material, see Table I. Accordingly, in the fine model the mesh size used for the multiphysics analysis is higher compared to the one used for the discretisation of the EM problem alone.

We homogenise (4) applying the multiple-scales (MS) method [15]. We introduce  $\mathbf{x}' = \mathbf{x}/\tau$  as the microscale variable that measures variations within a periodic cell, where  $\tau = \frac{l}{W} \ll 1$ ,  $W$  is the reference macroscale length and  $l$  the separation between the conductors (see Fig. 1);  $\mathbf{x}$  is the macroscale variable accounting for variations in the whole slot. As usual in the MS method, we assume  $\mathbf{x}'$  to be independent from  $\mathbf{x}$  and impose that the solution is exactly periodic in  $\mathbf{x}'$ . After introducing the two scales and using the chain rule, spatial derivatives transform according to  $\nabla_{\mathbf{x}} \rightarrow \nabla_{\mathbf{x}} + \frac{1}{\tau} \nabla_{\mathbf{x}'}$ . With this transform the dimensionless form of (4) becomes

$$\tau^2 \alpha_m \frac{\partial \tilde{T}}{\partial \tilde{t}} = \beta_m \left( \tau^2 \nabla_{\tilde{\mathbf{x}}}^2 \tilde{T} + 2\tau \nabla_{\tilde{\mathbf{x}}} \cdot \nabla_{\tilde{\mathbf{x}'}} \tilde{T} + \nabla_{\tilde{\mathbf{x}'}}^2 \tilde{T} \right) + \tau^2 \tilde{\dot{q}} \quad (5)$$

where tilde denotes non-dimensional variables, e.g.  $\mathbf{x} = \hat{x}\tilde{\mathbf{x}}$  with  $\hat{x} = W$ , and the following dimensionless groups were introduced

$$\alpha_m = \frac{W^2}{\tilde{t}} \frac{c_m d_m}{\hat{k}}, \quad \beta_m = \frac{k_m}{\hat{k}}$$

where the subscript  $m$  refers to each material part of the winding compound:  $c$  for the conductor,  $i$  insulation and  $ep$  epoxy (see Table I);  $\tilde{t}$  is a reference time,  $\tilde{\dot{q}}$  the nondimensional heat generation and  $\hat{k}$  the reference thermal conductivity, e.g.  $\hat{k} = k_{ep}$ .

Following the standard MS method, we now seek an asymptotic solution in the limit of small  $\tau$  to (5) of the form  $\tilde{T}(\tilde{\mathbf{x}}', \tilde{\mathbf{x}}, \tilde{t}) = \tilde{T}^{(0)}(\tilde{\mathbf{x}}', \tilde{\mathbf{x}}, \tilde{t}) + \tau \tilde{T}^{(1)}(\tilde{\mathbf{x}}', \tilde{\mathbf{x}}, \tilde{t}) + \tau^2 \tilde{T}^{(2)}(\tilde{\mathbf{x}}', \tilde{\mathbf{x}}, \tilde{t}) + \dots$ , periodic in  $\tilde{\mathbf{x}'}$ . Performing an asymptotic analysis of (5) up to  $o(\tau^2)$  we obtain the following homogenised heat equation

$$\tilde{C}_{eq} \frac{\partial \tilde{T}^{(0)}}{\partial \tilde{t}} = \nabla_{\tilde{\mathbf{x}}} \cdot \left( \tilde{k}_{eq} \nabla_{\tilde{\mathbf{x}}} \tilde{T}^{(0)} \right) + \tilde{\dot{q}}_{eq} \quad (6a)$$

where  $\tilde{C}_{eq}$  is the effective heat capacity,  $\tilde{k}_{eq}$  the  $2 \times 2$  effective thermal conductivity matrix and  $\tilde{\dot{q}}_{eq}$  the equivalent

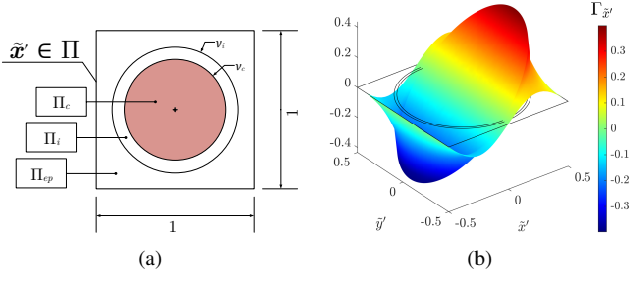


Fig. 4. (a) Microscopic domain  $\tilde{\mathbf{x}}' \in \Pi$  related to the square lattice wires,  $\nu_c = \frac{r_c}{l}$  and  $\nu_i = \frac{r_i}{l}$ , and (b)  $\Gamma_{\tilde{\mathbf{x}}'}$  distribution for a square lattice configuration with  $\lambda = 0.6$

non-dimensional heat generation, defined as

$$\tilde{C}_{eq} = \frac{1}{\Pi} \sum_m \alpha_m \Pi_m \quad (6b)$$

$$\tilde{k}_{eq} = \frac{1}{\Pi} \sum_m \left[ \beta_m \int_{\Pi_m} \mathbf{I}_d - \mathbf{F}(\tilde{\mathbf{x}}') \right] d\Pi_m \quad (6c)$$

$$\dot{\tilde{q}}_{eq} = \lambda \dot{\tilde{q}} \quad (6d)$$

where in (6c)  $\mathbf{I}_d$  is the  $2 \times 2$  identity matrix,  $(\mathbf{F})_{ij} = \partial \Gamma_j / \partial \tilde{x}'_i$  the transpose of the Jacobian matrix of  $\Gamma$ , and  $\Pi_m$  represents a surface according to Fig. 4(a) ( $\Pi_c \cup \Pi_i \cup \Pi_{ep} = 1$ ).

$\Gamma$  is a vector function whose components  $\Gamma_r$  ( $r = \tilde{x}', \tilde{y}'$ ) satisfy the following problem in the cell domain of Fig. 4(a)

$$\beta_m \nabla_{\tilde{\mathbf{x}}'}^2 \Gamma_r = 0 \quad (7a)$$

$$\beta_c (\nabla_{\tilde{\mathbf{x}}'} \Gamma_r - \mathbf{e}_r) \cdot \mathbf{n} = \beta_i (\nabla_{\tilde{\mathbf{x}}'} \Gamma_r - \mathbf{e}_r) \cdot \mathbf{n} \quad \text{on} \quad \|\tilde{\mathbf{x}}'\| = \nu_c, \quad (7b)$$

$$\beta_i (\nabla_{\tilde{\mathbf{x}}'} \Gamma_r - \mathbf{e}_r) \cdot \mathbf{n} = \beta_f (\nabla_{\tilde{\mathbf{x}}'} \Gamma_r - \mathbf{e}_r) \cdot \mathbf{n} \quad \text{on} \quad \|\tilde{\mathbf{x}}'\| = \nu_i \quad (7c)$$

with  $\Gamma_r$  periodic on the external boundaries, and  $\mathbf{e}_r$  is the unit vector in the  $r$ th direction in  $\Pi$ . The unit cell of Fig. 4(a) is obtained by nondimensionalising the original cell with respect to  $l$ , e.g.  $\nu_c = \frac{r_c}{l}$  and  $\nu_i = \frac{r_i}{l}$ . In Fig. 4(b) we show the solution of the cell problem for  $\Gamma_{\tilde{\mathbf{x}}'}$  that allows us to evaluate the effective thermal conductivity along  $x$  in the macroscopic domain using (6c). The method can be applied to any wire shape simply by setting the cell problem (7) accordingly.

Once the dimensions to  $\tilde{C}_{eq}$  and  $\tilde{k}_{eq}$  are restored, we obtain the parameters  $C_{eq}$  and  $k_{eq}$ . For instance, making reference to the material properties in Table I,  $\lambda = 0.6$  ( $r_c = 0.8 \times 10^{-1}$  m and  $r_i = 0.835 \times 10^{-1}$  m) and square lattice configuration, we obtain  $C_{eq} = 3.176$  MJ/m<sup>3</sup>K and  $k_{eq}$  is a  $2 \times 2$  diagonal matrix with  $k_{eq,j,j} = 2.53$  W/mK, due to the circular geometry.

#### IV. APPLICATION EXAMPLE

##### A. Internal heat generation

One of the inputs to the thermal model of the winding is the internal heat generation due to the circulating currents. In the fine model the magnitude of the internal heat generation can be estimated very accurately by evaluating the real part

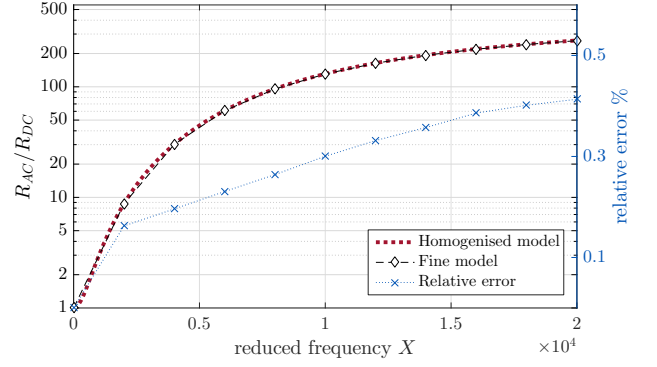


Fig. 5. Evaluation of ac losses in the slot of Fig. 1 in terms of the ratio  $R_{AC}/R_{DC}$  at various frequencies with the fine and homogeneous model, with relative error

of  $S$ ,  $P = Ln_w \int_{\Omega_c} \rho |J|^2 d\Omega$ . For the homogenised model we evaluate the real parts of (2)

$$P_h = p_I R_{DC} |I|^2 + p_B \frac{\lambda r^2 \omega^2 L}{4\rho} \sum_w \left( \int_{\Omega} |b|^2 d\Omega_w \right) \quad (8)$$

since in the homogenised winding we impose a uniform current density  $|J_h| = \frac{\lambda |I|}{\pi r^2}$  [7] and  $\Omega_w$  is the surface of the  $w$ th conductor in the slot.

By way of example, we compare the fine and homogenised models in estimating the losses, applying the approaches to the reference electrical machine open slot shown in Fig. 1. The geometry and dimensions are given in Fig. 1 with the material properties of Table I. For this case study we assume the core (M19) to be linear and lossless (constant real-valued permeability) as the focus of this analysis is on the winding domain.

We feed the winding with a sinusoidal current with  $|I| = 1$  A at various frequencies. In this first analysis, we assume the EM and thermal problems to be decoupled, using a fixed electrical conductivity  $\rho = \rho(20^\circ\text{C})$ . The losses, expressed as usual in terms of the ratio  $R_{AC}/R_{DC}$ , where  $R_{AC} = P/|I|^2$  is the equivalent  $R_{AC}$  resistance, are presented for the two models in Fig. 5. The agreement between the two models is very good, with a relative error lower than 0.5%.

It is now interesting to look at the loss distribution within the winding domain. At low frequencies the ac effects are minimal, Fig. 5, and the losses are almost uniformly distributed between the wires. Increasing the frequency, the leakage flux due to the slot opening produces high proximity losses in the wires at the top of the winding domain. In Fig. 6 we compare the estimation of the loss distribution in the fine and homogenised winding domains at  $X = 1$  ( $f = 6.65$  kHz) and  $|I| = 3$  A. The fine model, Fig. 6(a), provides a very accurate distribution of the losses within each wire, with the highest peaks in the wires sitting in the top corners. On the other hand, the homogenised model, Fig. 6(b), gives the macroscopic loss distribution. The peaks are still located in the top corners, however the maximum values are significantly lower since we lose information about the wire geometry (although in a cell-average sense the losses are correct).

The equivalence of the two loss profiles can be proved

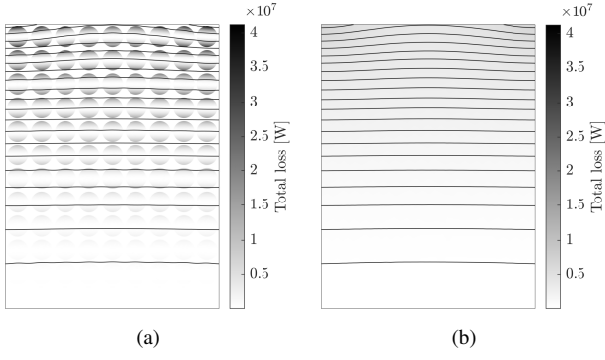


Fig. 6. Estimation of the total loss and magnetic flux lines in the winding domain at  $X = 1$  ( $f = 6.65$  kHz,  $|I| = 3$  A) with (a) the fine model and (b) the homogenised model. Wires distributed on a square lattice with  $\lambda = 0.6$  and constant electrical resistivity  $\rho = \rho(20^\circ\text{C})$

by analysing the output temperature fields of the fine and homogenised thermal problems using the losses of Fig. 6. For the thermal problem we look at the steady state temperature distribution imposing the boundary conditions shown in Fig. 1, where  $T_{fixed} = 20^\circ\text{C}$  and the convection is modelled with the law  $\dot{q}_{conv} = h(T - T_\infty)$ , where  $h = 20 \text{ W m}^{-2}\text{K}^{-1}$  and  $T_\infty = 20^\circ\text{C}$ ; thermal periodicity is imposed on the lateral edges. These boundary conditions can be representative of a machine cooled with a water jacket. The results are presented in Fig. 7. In the fine model the temperature within each conductor is uniform, Fig. 7(a). The homogenised model is able to capture quite accurately the hot-spot temperature magnitude and location, Fig. 7(b), as confirmed in Fig. 7(c) where we plot the  $T$  profile along the vertical mid-cross section within the winding domain; in Fig. 7(c) the difference between the hot-spot temperatures using both approaches, defined as the highest temperature in the winding domain, is lower than  $0.1^\circ\text{C}$ .

### B. Internal heat generation including temperature effects

As mentioned in the previous sections, temperature affects the electrical resistivity of the conductors according to (3). The temperature dependence of the resistivity  $\rho$  cannot be neglected for a proper assessment of the losses and the hot-spot temperature [4]. In the fine model this can be easily included by solving the model iteratively for  $\rho(T)$ . As shown in Section II, the parameters  $p_I$ ,  $q_I$ ,  $p_B$  and  $q_B$  vary with temperature for a certain  $f$ . Using a single set of parameters, temperature dependency can be captured with  $X(T) = r\sqrt{f\pi\mu_0/\rho(T)}$ , leading to a new formulation of the effective complex reluctance

$$\nu_{prox}(\mathbf{x}, T) = q_B(X(T))\nu_0 + j p_B(X(T)) \frac{\lambda r^2 \omega}{4\rho(T)} \quad (9a)$$

and effective impedance

$$Z_{skin}(\bar{T}) = p_I(X(\bar{T}))R_{DC}(\bar{T}) + j q_I(X(\bar{T}))\omega \frac{\mu_0 L}{8\pi\lambda} \quad (9b)$$

where  $\bar{T}$  is the average temperature in the winding domain. In (9b) we used the average temperature  $Z_{skin}(\bar{T})$  since

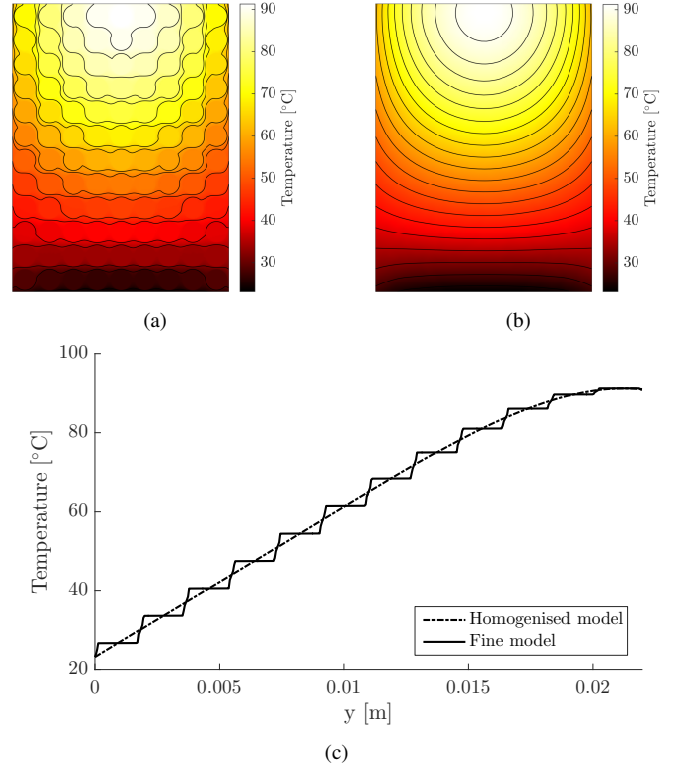


Fig. 7. Estimation of the temperature distribution in the winding domain at  $X = 1$  ( $f = 6.65$  kHz,  $|I| = 3$  A) with (a) the fine model and (b) the homogenised model. (c) Comparison of the solution along the vertical mid-cross section within the winding domain. The solutions are obtained using losses generated by the EM fine and homogenised model respectively (Fig. 6)

the impedance is an element placed in the external lumped circuit. This assumption, however, has a small impact on the model accuracy since in general with increasing frequency the skin effect is almost negligible compared to the proximity effect when we have leakage flux [7,10]. On the other hand,  $\nu_{prox}(\mathbf{x}, T)$  varies with the macroscale coordinate  $\mathbf{x}$  within the homogenised winding domain.

In Fig. 8 we present the loss estimation with the coupled EM and thermal model in terms of  $R_{AC}/R_{DC}$ , referring to the same case study of Fig. 1. The ratio  $R_{AC}/R_{DC}$  is now plotted against  $f$  because  $X(T)$  cannot be uniquely defined. Compared to the decoupled model with constant conductivity  $\rho = \rho(20^\circ\text{C})$ , the coupled model gives lower ac losses. To evaluate different thermal gradients within the winding we change the feeding current, namely  $|I| = 1, 3, 5$  A. A higher temperature and, accordingly, a higher resistivity, opposes the circulation of eddy currents which in turn means lower ac losses. As a consequence, the hot-spot temperature is lower when we couple the EM and thermal problems in this particular scenario. This is confirmed in Fig. 9(a), where we plot the temperature along the vertical mid-cross section within the winding for a feeding current  $|I| = 5$  A at  $f = 5$  kHz. The match between the fine and homogenised models is again very good. Using an Intel i7 (3.2 GHz and 32 Gb RAM) the solution takes 174 s for the fine model ( $2.17 \times 10^5$  elements) and 3 s for the homogenised model ( $2 \times 10^3$  elements).



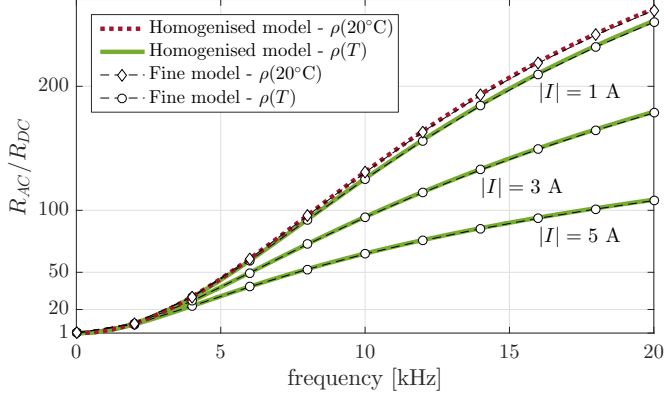


Fig. 8. Evaluation of ac losses in the slot of Fig. 1 in terms of the ratio  $R_{AC}/R_{DC}$  at various frequencies with the fine and homogeneous model, with and without temperature coupling

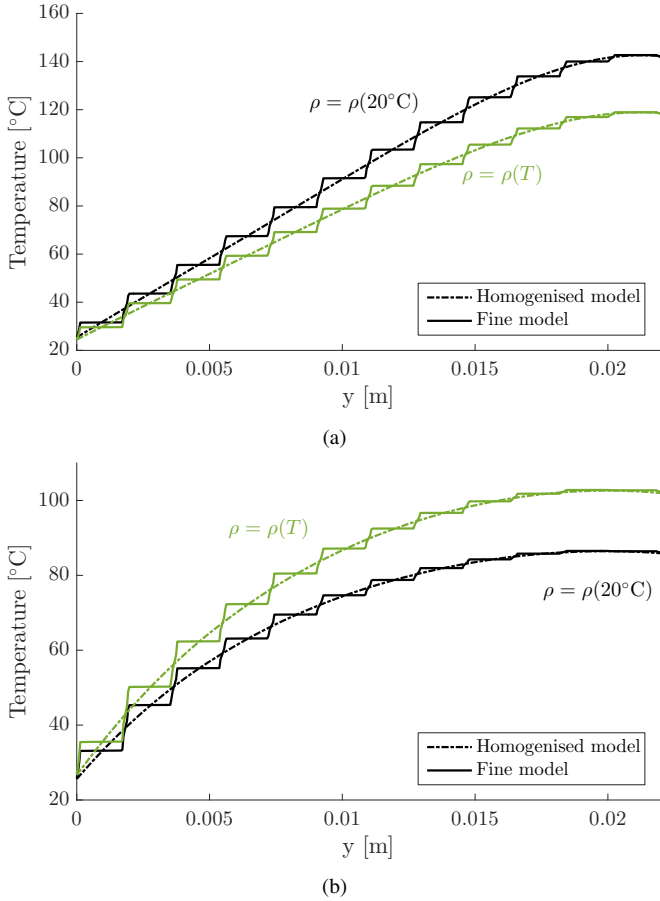


Fig. 9. Comparison of the temperature distribution along the vertical mid-cross section within the winding domain for the fine and homogenised models with  $\rho(20^\circ\text{C})$  and  $\rho(T)$  for the case (a)  $|I| = 5\text{ A}$  at  $f = 5\text{ kHz}$  and (b)  $|I| = 30\text{ A}$  at  $f = 100\text{ Hz}$

At low frequencies the solution of the coupled EM-thermal problem leads to a higher hot-spot temperature. This is because the ac effects are smaller and the temperature dependence of  $\rho$  implies higher  $R_{DC}$ . This is shown in Fig. 9(b) where we compare the temperature estimation with  $\rho(20^\circ\text{C})$  or  $\rho(T)$  with a feeding current  $|I| = 30\text{ A}$  at  $f = 100\text{ Hz}$ . In all the temperature profiles of Fig. 9 the difference in the estimation of the hot-spot is within  $0.1^\circ\text{C}$  between the homogenised and fine model.

Fig. 9 helps to highlight how different loss profiles influence the temperature field. The results of Fig. 9(b) refer to the case of uniformly distributed losses. Here, the solution given by the homogenised model can be approximated with a quadratic function. On the contrary, at high frequencies the losses are concentrated in the neighbourhood of the slot opening, due to the proximity effect. Accordingly the thermal gradient is linear far from the loss concentration. Therefore, assuming uniformly distributed losses  $P_h = R_{AC}|I|^2$  in a thermal model under these conditions leads to an incorrect temperature distribution.

## V. CONCLUSION

In this paper we presented an original multiphysics homogenisation of an electrical machine slot, coupling EM and thermal homogenisation techniques for the estimation of conduction losses and the related temperature distribution. The method was applied to a reference electrical machine open slot. The results obtained after the homogenisation are in very good agreement compared to a fine model (hot-spot  $\Delta T < 0.1^\circ\text{C}$ ), over a wide range of frequencies. As shown in this paper, a multiphysics analysis is necessary for a proper assessment of the losses and the hot-spot temperature. This coupled analysis is made computationally affordable with the use of the proposed multiphysics homogenisation. Moreover, the temperature distribution given by the fine model can be reconstructed from the homogenised model by post-processing the solution.

The method can be applied to any symmetrical wire shape and periodic wire distribution or to different applications, such as transformers, magnetic components in power electronics, or actuators. This is confirmed by the high accuracy of the method over a wide range of frequencies. The technique presented in this paper can be extended to include non-steady state behaviour, or to 3D geometries including for example the homogenisation of laminations for an efficient estimation of the flux distribution in the core at high frequencies. It could be also interesting to employ the MS method, here used for the thermal homogenisation, to the EM problem.

## REFERENCES

- [1] K. N. Gyftakis, D. F. Kavanagh, M. Sumislawska, D. A. Howey, and M. McCulloch, "Dielectric characteristics of electric vehicle traction motor winding insulation under thermal ageing," *IEEE Transactions on Industry Applications*, vol. 52, no. 2, pp. 313–318, 2016.
- [2] R. Wrobel, A. Mlot, and P. H. Mellor, "Contribution of End-Winding Proximity Losses to Temperature Variation in Electromagnetic Devices," *IEEE Transactions on Industrial Electronics*, vol. 59, no. 2, pp. 848–857, 2012.
- [3] P. Mellor, R. Wrobel, and N. Simpson, "AC Losses in High Frequency Electrical Machine Windings formed from Large Section Conductors," in *Energy Conversion Congress and Exposition (ECCE)*, no. 2, 2014, pp. 5563–5570.

- [4] R. Wrobel, D. E. Salt, A. Griffo, N. Simpson, and P. H. Mellor, "Derivation and scaling of AC copper loss in thermal modeling of electrical machines," *IEEE Transactions on Industrial Electronics*, vol. 61, no. 8, pp. 4412–4420, 2014.
- [5] D. Cioranescu and J. S. J. Paulin, *Homogenization of reticulated structures*. Springer Science & Business Media, 2012.
- [6] O. Moreau, L. Popiel, and J. L. Pages, "Proximity losses computation with a 2D complex permeability modelling," *IEEE Transactions on Magnetics*, vol. 34, no. 5 PART 1, pp. 3612–3615, 1998.
- [7] J. Gyselinck and P. Dular, "Frequency-domain homogenization of bundles of wires in 2-D magnetodynamic FE calculations," *IEEE Transactions on Magnetics*, vol. 41, no. 5, pp. 1416–1419, 2005.
- [8] J. Gyselinck, R. V. Sabariego, and P. Dular, "Time-Domain Homogenization of Windings in 2-D Finite Element Models," *IEEE Transactions on Magnetics*, vol. 43, no. 4, pp. 1297–1300, 2007.
- [9] R. V. Sabariego, P. Dular, and J. Gyselinck, "Time-domain homogenization of windings in 3-D finite element models," *IEEE Transactions on Magnetics*, vol. 44, no. 6, pp. 1302–1305, 2008.
- [10] J. Gyselinck, P. Dular, N. Sadowski, P. Kuo-Peng, and R. Sabariego, "Homogenization of Form-Wound Windings in Frequency and Time Domain Finite-Element Modeling of Electrical Machines," *IEEE Transactions on Magnetics*, vol. 46, no. 8, pp. 2852–2855, 2010.
- [11] F. Chauvicourt, P. Romanazzi, D. Howey, A. Dziechciarz, C. Martis, and C. T. Faria, "Review of Multidisciplinary Homogenization Techniques applied to Electric Machines," in *Eleventh International Conference on Ecological Vehicles and Renewable Energies (EVER)*, Monaco, 2016.
- [12] Z. Hashin and S. Shtrikman, "A variational approach to the theory of the elastic behaviour of multiphase materials," *Journal of the Mechanics and Physics of Solids*, vol. 11, no. 2, pp. 127–140, 1963.
- [13] N. Simpson, R. Wrobel, and P. H. Mellor, "Estimation of Equivalent Thermal Parameters of Impregnated Electrical Windings," *IEEE Transactions on Industry Applications*, vol. 49, no. 6, pp. 2505–2515, 2013.
- [14] R. Wrobel and P. H. Mellor, "A General Cuboidal Element for Three-Dimensional Thermal Modelling," *IEEE Transactions on Magnetics*, vol. 46, no. 8, pp. 3197–3200, aug 2010.
- [15] E. Sanchez-Palencia, *Non-homogeneous media and vibration theory*. Springer-Verlag, 1980.
- [16] J. A. Ferreira, "Improved Analytical Modeling of Conductive Losses in Magnetic Components," *IEEE Transactions on Power Electronics*, vol. 9, no. 1, pp. 127–131, 1994.
- [17] K. Niyomsatian, J. V. den Keybus, R. V. Sabariego, and J. Gyselinck, "Frequency-Domain Homogenization for Impedance Characterization of Litz-Wire Transformers in 2-D Finite Element Models," in *Eleventh International Conference on Ecological Vehicles and Renewable Energies (EVER16)*, 2016.

**Pietro Romanazzi** received the Bachelor's and Master's Degree in Mechanical Engineering from the University of Udine, Udine, Italy, in 2009 and 2011 respectively. From 2014 he is an EC sponsored Marie Curie early stage researcher within the ADEPT project ([www.adept-itn.eu](http://www.adept-itn.eu)) pursuing the D.Phil. degree at University of Oxford, Oxford, U.K.

**Johan Gyselinck** (M'05) received the M.S. degree in electrical and mechanical engineering and the Ph.D. degree in applied sciences from Ghent University, Gent, Belgium, in 1991 and 2000, respectively. From 2000 to 2004, he was a Postdoctoral Researcher at the Applied and Computational Electromagnetics research unit of the University of Liège, Liège, Belgium. He is currently an Associate Professor with the Université Libre de Bruxelles, Brussels, Belgium, and his research mainly concerns the numerical computation of magnetic fields, the simulation and control of electrical machines and drives, and renewable energy systems.

**Maria Bruna** received the Master's Degrees in Mathematics and Industrial Engineering from the Universitat Politècnica de Catalunya, Barcelona, Spain, in 2007 and 2008 respectively, and the M.Sc. in Mathematical Modelling and Scientific Computing and the D.Phil. in Applied Mathematics from the University of Oxford, Oxford, U.K., in 2008 and 2012 respectively. She currently holds a Junior Research Fellowship in Mathematics at St John's College, Oxford, and is a member of the Mathematical Institute at the University of Oxford. Her research interests include stochastic modelling and homogenisation techniques in the areas of mathematical biology and industrial mathematics.

**David A. Howey** (M'10) received the B.A. and M.Eng. degrees from Cambridge University, Cambridge, U.K., in 2002, and the Ph.D. degree in thermal design of electrical machines from Imperial College London, London, U.K., in 2010. He is currently an Associate Professor with the Energy and Power Group, Department of Engineering Science, University of Oxford, Oxford, U.K. He leads projects on fast electrochemical modelling, model-based battery management systems, battery thermal management, battery degradation and motor thermal management and degradation. His research interests include condition monitoring and management of electric-vehicle components.